Self-assembly 2D zinc-phthalocyanine heterojunction: An ideal platform for high efficiency solar cell

Xue Jiang, Zhou Jiang, and Jijun Zhao

Citation: Appl. Phys. Lett. **111**, 253904 (2017); doi: 10.1063/1.5005119
View online: https://doi.org/10.1063/1.5005119
View Table of Contents: http://aip.scitation.org/toc/apl/111/25
Published by the American Institute of Physics

Articles you may be interested in

Spin-phonon coupling in antiferromagnetic nickel oxide
Applied Physics Letters **111**, 252402 (2017); 10.1063/1.5009598

Nanoparticle detection in an open-access silicon microcavity
Applied Physics Letters **111**, 253107 (2017); 10.1063/1.5008492

Enhanced recoverable energy storage density and high efficiency of $SrTiO_3$-based lead-free ceramics
Applied Physics Letters **111**, 253903 (2017); 10.1063/1.5000980

Chemical vapour deposition of freestanding sub-60 nm graphene gyroids
Applied Physics Letters **111**, 253103 (2017); 10.1063/1.4997774

Burying non-radiative defects in InGaN underlayer to increase InGaN/GaN quantum well efficiency
Applied Physics Letters **111**, 262101 (2017); 10.1063/1.5007616

Temperature-dependent transport properties of graphene decorated by alkali metal adatoms (Li, K)
Applied Physics Letters **111**, 263502 (2017); 10.1063/1.5001080

AIP | Conference Proceedings
Get 30% off all print proceedings!
Enter Promotion Code PDF30 at checkout

Self-assembly 2D zinc-phthalocyanine heterojunction: An ideal platform for high efficiency solar cell

Xue Jiang,[1] Zhou Jiang,[1] and Jijun Zhao[1,2,a)]
[1]*Key Laboratory of Materials Modification by Laser, Ion and Electron Beams (Dalian University of Technology), Ministry of Education, Dalian 116024, China*
[2]*Beijing Computational Science Research Center, Beijing 100089, China*

(Received 17 September 2017; accepted 14 November 2017; published online 20 December 2017)

As an alternative to silicon-based solar cells, organic photovoltaic cells emerge for their easy manufacture, low cost, and light weight but are limited by their less stability, low power conversion efficiencies, and low charge carrier mobilities. Here, we design a series of two-dimensional (2D) organic materials incorporating zinc-phthalocyanine (ZnPc) based building blocks which can inherit their excellent intrinsic properties but overcome those shortcomings. Our first-principles calculation shows that such 2D ZnPc-based materials exhibit excellent thermal stabilities, suitable bandgaps, small effective masses, and good absorption properties. The additional benzene rings and nitrogen atoms incorporated between ZnPc molecules are mainly responsible for the modifications of electronic and optical properties. Moreover, some heterojunction solar cells constructed using those 2D ZnPc monolayers as the donor and acceptor have an appropriate absorber gap and interface band alignment. Among them, a power conversion efficiency up to 14.04% is achieved, which is very promising for the next-generation organic solar cells. *Published by AIP Publishing.*
https://doi.org/10.1063/1.5005119

Photovoltaics (PV) is a well-established method for converting energy radiated from sun into electricity. There are two kinds of PV technologies: inorganic PV and organic PV. The advantage of the former ones is the efficiency, which has exceeded 25%, 20%, and 44% for single-crystalline silicon, multi-crystalline silicon, and multi-junction solar cells,[1] respectively. However, inorganic PV technologies suffer from the shortcomings of high costs of production and installation, heavy weight, and toxicity of the active materials. The latter ones, organic PV technologies mainly focusing on conjugated polymers and small molecules, stand out for their easy manufacture, low cost, and light weight. Their tunable properties and strong optical absorption are also beneficial to solar cell applications. However, their long-term stability, power conversion efficiency (PCE), and charge carrier mobilities are still much lower than their inorganic counterparts.[1] It is desirable to search suitable semiconductor materials that inherit the excellent intrinsic advantages of both inorganic and organic PV materials but overcome their shortcomings.

Two-dimensional (2D) organic materials are fantastic choices to fulfill the criteria for donors/acceptors in the solar cell. They are a class of porous crystalline materials constructed by the linkage of organic secondary building blocks through metal or covalent nodes to produce predetermined structures, such as 2D metal organic frameworks (MOFs), 2D covalent organic frameworks (COFs), and 2D conjugated polymers. Based on reticular chemistry,[2,3] those 2D organic materials possess the high-quality genes of the organic PV materials. That is, their electronic and optical properties are mainly determined by the building polymers and small molecules. Most importantly, 2D organic materials prevail polymers and small organic molecules by the excellent long-term thermal stability and band-like transport behavior owing to their crystalline nature. An exciting breakthrough in 2D organic material preparation technology has been achieved by Abel *et al.*[4] Using the molecular self-assembly method, they have synthesized a single layer of Fe-phthalocyanine on an insulating substrate, which is crucial to transfer the 2D organic materials to devices by preserving their intrinsic properties. Thus, it is naturally to expect that high-efficiency 2D organic PV materials can be constructed from suitable photoactive ligands.

Among countless photoactive ligands, phthalocyanine (Pc) and its metalloderivatives,[5] which are 18 π electron aromatic porphyrin synthetic analogues consisting of four isoindole subunits linked together through nitrogen atoms, stand out since their flat and rigid configurations are feasible to form continuous 2D networks by supramolecular self-assembly. In fact, phthalocyanine is reported as the first organic semiconductor exhibiting the PV effect and holds some advantages like high stability, rich redox chemistry, and high LUMO energy, which are superior to the other polymers.[6] There are many other undeniable signatures relevant to the application of solar cells: (i) Phthalocyanines exhibit very high extinction coefficients in the wavelength range of 600–800 nm where the maximum of solar photon flux occurs for the efficient photon harvesting;[1] (ii) The diffusion length of zinc adopted Pcs is very long and can reach 30 nm;[7] (iii) Phthalocyanines exhibit excellent *p*-type and *n*-type semiconducting behaviors simultaneously. Therefore, a critical question arises: how to design high-efficiency 2D organic PV materials by taking advantage of the phthalocyanine ring?

Using first-principles calculations, here we design a series of stable 2D organic photovoltaic candidates with Zn embedded phthalocyanine (ZnPc) rings as organic linkers. Most of them possess direct bandgap (ca. 1.0 eV) and good

a)Author to whom correspondence should be addressed: zhaojj@csrc.ac.cn

absorption properties and provide an effective strategy for assembling phthalocyanine rings into donor/acceptor based photovoltaic cells. We further blend those donor and acceptor 2D ZnPc species together into a bilayer solar cell. Their small lattice mismatch, suitable absorber bandgap, and donor-acceptor interface band alignment result in promising PCE in the range of 7–14% that depends on the different combinations.

The structures and electronic properties of all 2D ZnPcs were investigated using density functional theory (DFT) calculations. The Vienna *ab initio* simulation package (VASP)[8] in association with projector augmented wave (PAW) potentials[9] within the generalized gradient approximation (GGA) of Perdew-Burke-Ernzerhof (PBE) exchange-correlation parameterization[10] was used. The cutoff for the planewave basis was 800 eV, and a $5 \times 5 \times 1$ grid was used for **k**-point sampling. 2D ZnPcs were simulated by slab models with a vacuum thickness of 15 Å. For each 2D ZnPc, the in-plane lattice parameters and atomic coordinates are fully optimized with the convergence criteria of 0.01 meV and 0.001 eV/Å for the total energy and force, respectively. For the monolayer 2D ZnPcs with PBE-optimized geometries, a hybrid Heyd-Scuseria-Ernzerhof (HSE06) functional[11] was further used to evaluate the bandgap and optical properties more accurately. Based on the Kramers-Kronig dispersion relation,[12] optical absorption spectra of the 2D ZnPcs were computed from the imaginary part of dielectric function. *Ab initio* molecular dynamics (AIMD) simulations[13] (with 1 fs time step) were performed to evaluate the thermal stability of 2D ZnPc structures at room temperature. Following the method by Seiji *et al.*,[14] the work function was evaluated by the difference between electrostatic potential in a vacuum region and the Fermi energy.

Inspired by the reticular chemistry and the recently synthesized phthalocyanine dimers, trimers, tetramers,[5] 1D phthalocyanine arrays, and 2D Fe-Pcs,[4] we extend those phthalocyanine systems to a series of unprecedented 2D periodic networks to explore their organic PV applications. In principle, many possible 2D ZnPcs can be constructed by properly designing the functionalized phthalocyanines and template.[15] As shown in Fig. 1 and S1 (supplementary material), the adjacent phthalocyanine rings of 2D ZnPc-1, 2D ZnPc-2, 2D ZnPc-3, 2D ZnPc-4, and 2D ZnPc-5 are connected by sharing annulated benzene, naphthalene, and anthracene or incorporation of nitrogen atoms in the benzene units, respectively. The essential idea of designing these 2D ZnPcs is to screen out feasible raw reactants and reactions. Moreover, the bandgap and optical transition energy have to be considered to utilize the solar light effectively. Among over 70 reported metal atoms, the embedded atom is restricted to zinc here to avoid possible spin polarization and simplify our theoretical calculations. However, 2D phthalocyanines with other metal atoms also broaden the database of 2D organic photovoltaic materials for further screening.

The space group, equilibrium lattice constant, and key parameters for electronic properties of these newly constructed 2D ZnPc models are summarized in Table I. All these 2D ZnPcs present a tetragonal/orthogonal symmetry with the lattice constant ranging from 10.605 Å to 15.675 Å. Upon relaxation, no in-plane and out-plane distortions are

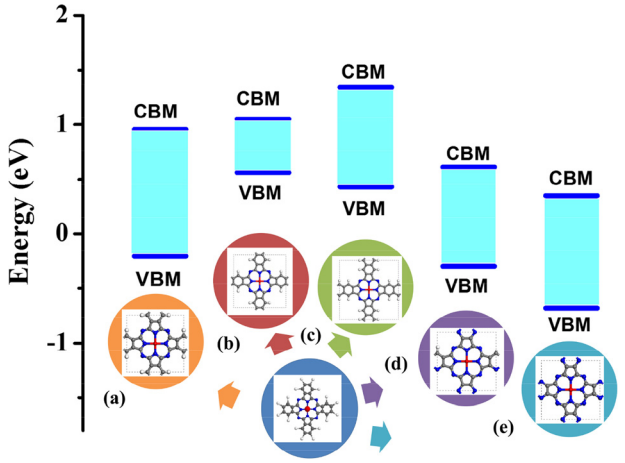


FIG. 1. Geometries and CBM and VBM positions of 2D ZnPc-1, 2D ZnPc-2, 2D ZnPc-3, 2D ZnPc-4, and 2D ZnPc-5 from HSE06 calculations. The reference potential is the vacuum level. The grey, blue, white, and red atoms are C, N, H, and Zn, respectively.

observed. Meanwhile, zinc-nitrogen bond distances in each 2D ZnPc system are equal (Fig. 1 and Table I), indicating that the zinc atoms perfectly sit at the center of the phthalocyanine framework. Good structural stability of these 2D ZnPcs is also demonstrated by their binding energy (E_b) in the range of 7.67–8.37 eV (Table S1, supplementary material). For comparison, 2D FePcs,[4] certified stable organic materials, possess a comparable binding energy of 8.19 eV. The thermal stabilities have been assessed by AIMD simulations. As shown in Fig. S2 (supplementary material), the 2D ZnPc structures remain nearly planar throughout the simulation period (up to 20 ps), and their energy fluctuations in the range of only 0.1–0.2 eV/atom at 300 K are quite acceptable for the 2D organic materials.[16] Their feasibility of chemical preparation in experiments is suggested by five potential chemical reactions, which are displayed in Fig. S3 (supplementary material). Those satisfactory values of reaction heats suggest that our predicted 2D ZnPcs are feasible for experimental synthesis.

The valence band maximum (VBM) and conduction band minimum (CBM) levels of these 2D ZnPc systems from the HSE06 calculations are plotted in Fig. 1 and Table S2 (supplementary material). Both inserting additional benzene rings and substituting carbon atoms with nitrogen atoms have significant impacts on the absolute energy of the unoccupied state and occupied state, but they shift the energy level in different directions. Naphthalene and anthracene sharing in 2D ZnPcs (2D ZnPc-2 and 2D ZnPc-3) lift the CBM level up from that of benzene ring linked 2D ZnPc-1

TABLE I. The space group, zinc-zinc distance (L), zinc-nitrogen distance (D), bandgap (E_g), and wavelength of the Q band (λ) of 2D ZnPc-1, 2D ZnPc-2, 2D ZnPc-3, 2D ZnPc-4, and 2D ZnPc-5, respectively.

	Space group	L (Å)	D (Å)	E_g (eV)	λ (nm)
ZnPc-1	P4/MMM	10.748	2.001	1.16	689
ZnPc-2	P4/MMM	13.214	2.007	0.49	743
ZnPc-3	P4/MMM	15.675	2.008	0.92	899
ZnPc-4	AMM2	10.674	2.008	0.91	725, 1100
ZnPc-5	P4/MMM	10.605	2.01	1.03	569

by 0.1 eV and 0.39 eV, respectively. Meanwhile, the valence band edges of 2D ZnPc-2 and 2D ZnPc-3 also move to a higher energy range by 0.77 eV and 0.63 eV, respectively. Compared to 2D ZnPc-1, nitrogen doping in 2D ZnPc-4 and ZnPc-5 pushes the CBM (VBM) position down by 0.34 eV (0.09 eV) and 0.6 eV (0.47 eV), respectively. The difference in energy shift can be ascribed to the number of benzene rings and nitrogen atoms. That is, the VBM/CBM shifts of 2D ZnPc-5 (0.6 eV/0.47 eV) are larger than those of 2D ZnPc-4 (0.34 eV/0.09 eV). Anthracene sharing 2D ZnPc-3 (0.39 eV) can generally shift CBM positions strongly (0.1 eV), as compared to 2D ZnPc-2.

From the more accurate HSE06 calculations (Fig. S4, supplementary material), 2D ZnPc-1, 2D ZnPc-2, 2D ZnPc-3, 2D ZnPc-4, and 2D ZnPc-5 systems are all semiconductors with direct bandgaps of 1.16 eV, 0.49 eV, 0.92 eV, 0.91 eV, and 1.03 eV, respectively. In the 2D Brillouin Zone, both the CBM and VBM of 2D ZnPc-1, 2D ZnPc-2, 2D ZnPc-3, 2D ZnPc-4, and 2D ZnPc-5 locate at the Γ point, while the CBM and VBM of ZnPc-5 locate at the M point. By self-assembling phthalocyanine rings into 2D periodic networks, the originally flat bands become highly disperse, suggesting a better transport behavior. The corresponding effective masses of 2D ZnPc-1, 2D ZnPc-2, 2D ZnPc-3, 2D ZnPc-4, and 2D ZnPc-5 are listed in Table S3 (supplementary material). All these values are comparable to the conventional inorganic semiconductors such as silicon (0.13–0.96 m_e), gallium nitride (0.14–2.09 m_e), aluminum nitride (0.28–4.24 m_e), boron nitride (0.23–1.26 m_e), and silicon carbide (0.4–2.0 m_e).[17,18] For example, the hole effective mass in 2D ZnPc-4 along the [100] direction is 0.31 m_e, while the electron effective mass in 2D ZnPc-4 along the [100] direction is 0.69 m_e. Since the carrier mobility is inversely proportional to effective mass, the present 2D ZnPcs would have competitively high mobilities of the electron and hole. To further characterize the electron transport properties of these 2D ZnPcs, we calculated their carrier mobility within the deformation potential approximation.[19] The detailed results are presented in Table S4 (supplementary material). Except for ZnPc-2, the other four ZnPcs possess relatively large carrier mobilities. For example, the calculated electron and hole mobility of 2D ZnPc-1 are 400 $cm^2 V^{-1} S^{-1}$ and 1390 $cm^2 V^{-1} S^{-1}$, which are comparable to the theoretical value of MoS_2 (880 $cm^2 V^{-1} S^{-1}$).[20] The suitable bandgap together with good carrier mobility of those 2D ZnPcs suggests a preferable efficiency of light absorption and potential applications in optoelectronic devices. In fact, such promising results can be mainly attributed to the well-known merits of 2D organic materials:[21,22] (i) the chemical versatility and modularity of 2D organic materials endow them to form countless structures; (ii) their physical properties can be systematically controlled by carefully choosing their composition, structure, and functionality.

The simulated optical adsorption spectra of 2D ZnPc-1, 2D ZnPc-2, 2D ZnPc-3, 2D ZnPc-4, and 2D ZnPc-5 are displayed in Fig. 2. 2D ZnPc-1, 2D ZnPc-2, 2D ZnPc-3, and 2D ZnPc-5 show a well-resolved single absorption band due to their high symmetry, which is usually termed as the Q band and peaked at 689 nm, 743 nm, 899 nm, and 569 nm, respectively, while a split Q band (centered at 725 nm and

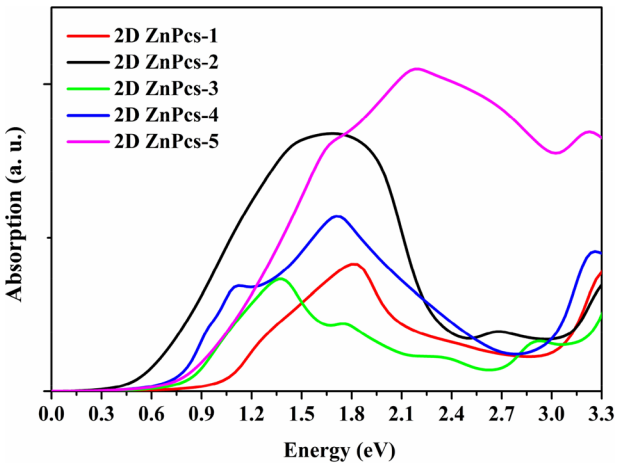


FIG. 2. Optical absorption spectra of 2D ZnPc-1, 2D ZnPc-2, 2D ZnPc-3, 2D ZnPc-4, and 2D ZnPc-5, respectively.

1100 nm) is observed in 2D ZnPc-4 as a result of its lower symmetry. In 2D ZnPc-4, one carbon atom in the benzene ring carries the hydrogen atom, whereas the nitrogen atom is not functionalized, giving two components of the split band in the x and y directions. In addition, Q bands are shifted drastically from phthalocyanine molecules to 2D period structures. For example, the Q band of our 2D ZnPc systems lies in the range of 589–899 nm, while the widely reported Q band for phthalocyanine molecules locates between 550 nm and 670 nm.[23] Similar to the electronic band structure, the extension of the π electron system and incorporation of the nitrogen content offer possibility to tailor the absorption properties of 2D ZnPc systems. In principle, the use of naphthalene and anthracene moieties instead of benzene groups generally leads to red shift in the Q band by 46–210 nm, which agrees well with the experimental observations of phthalocyanines (689 nm) and superphthalocyanine molecules at 750–945 nm.[24,25] One nitrogen atom in the benzene unit of the phthalocyanine causes a red-shifted Q band, whereas the absorption peak of two nitrogen incorporation (2D ZnPc-5) is higher than that of 2D ZnPc-1. In short, the absorption range of 2D ZnPcs can be tuned to a relatively wide visible range (569–1100 nm), which is very important to enhance the efficiency of solar cells. Among them, nitrogen doped ZnPC-5 seems to have a considerably higher absorption cross section in the UV region. Following such observation, B/O doping is also investigated; but unfortunately, no further enhancement in the absorption region has been found.

Besides suitable bandgap and good light absorption properties, exciton dissociation and charge separation are critical issues for the performance of solar cells. Stacking two 2D layered semiconductor materials into heterostructures provides a highly effective means to the manipulation of the charge carrier.[26–28] Compared to the single-layer 2D material, the 2D/2D stacked heterostructures possess rather larger surface area and abundant coupling heterointerfaces, which may easily facilitate the transfer and separation of photogenerated electron and hole pairs.[29] To design viable 2D ZnPc heterobilayers, two crucial requirements should be satisfied: (i) the donor and acceptor materials should have

similar lattice constants to reduce the mismatch; (ii) VBM/CBM energy difference of the two component materials should exhibit type II band alignment. For a type-II semiconductor/semiconductor heterojunction [Fig. 3(a)], the positions of valence and conduction band edges of component two is higher than those of component one, and the steps in the conduction and valence bands follow the same direction. Moreover, the difference of chemical potential between two semiconductor components induces a build-in electric field, which drives the photogenerated electrons and holes to move in opposite directions, leading to a spatial separation of the electrons and holes on different sides of the heterojunction.[30] Based on the calculated band alignments in Fig. 1, three 2D ZnPc/2D ZnPc interfaces can be selected from ten possible combinations, including 2D ZnPc-1/2D ZnPc-4, 2D ZnPc-1/2D ZnPc-5, and 2D ZnPc-4/2D ZnPc-5. The lattice mismatches for these three type II heterojunctions are all less than 1.3%. Moreover, we construct those 2D ZnPc heterojunctions with AA-stacking by aligning up the zinc atoms. The AA stacking mode maximizes the π-orbital overlap, which is favorable for charge transport. As displayed in Figs. 3(b) and 3(c), the localization of the electron and hole is clearly observed by their charge distributions.

Based on Scharber's finding,[31] the power conversion efficiency of those three type II heterojunctions, which is given by the open-circuit voltage (Voc) times the short-circuit current density (Jsc) times the electrical fill factor (FF) divided by the incident-light intensity, can be estimated as

$$\eta = \frac{0.65\left(E_g - \Delta E_c - 0.3\right)\int_{E_g}^{\infty} \frac{P(\hbar\bar{\omega})}{\hbar\bar{\omega}} d(\hbar\bar{\omega})}{\int_0^{\infty} P(\hbar\bar{\omega}) d(\hbar\bar{\omega})},$$

where the fill factor is taken as 0.65, and $P(\hbar\bar{\omega})$ is the AM1.5 solar energy flux at the photon energy $\hbar\bar{\omega}$. The optical bandgap of the 2D ZnPc donor (E_g) comes from our HSE06 calculations. The effective interface gaps ($E_g - \Delta E_c$) are calculated between the CBM level of the 2D ZnPc donors and the VBM level of the 2D ZnPc acceptors. To account for the energy conversion kinetics, the maximum open circuit voltage is estimated by the effective interface gap minus 0.3 eV.

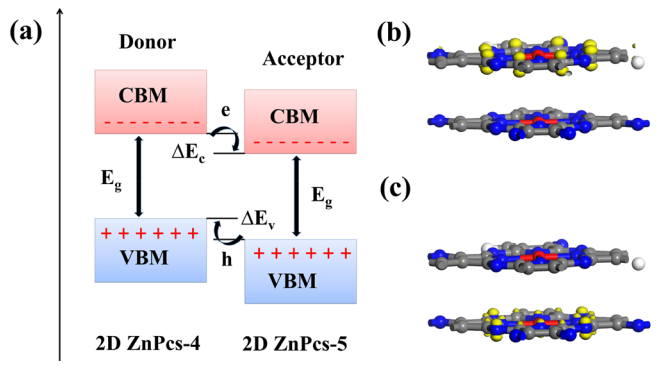


FIG. 3. (a) Schematic illustration of possible type-II donor-acceptor band alignments for the carrier transfer and separation in hybrid heterobilayers. E_g, ΔE_c, and ΔE_v are the bandgap, conduction band offsets, and valence band offsets, respectively; Charge distributions for electronic states at VBM (b) and CBM (c) of the 2D ZnPc-4/2D ZnPc-5 interface. The charge densities are plotted at an isovalue of 0.06 e.

As shown in Fig. 4, the 2D ZnPc-1/ZnPc-4 bilayer solar cell has a PCE of about 14.04%, the ZnPc-1/ZnPc-5 bilayer solar cell has a PCE of about 6.95%, and the ZnPc-4/ZnPc-5 bilayer solar cell has the potential to achieve a PCE of 11.77%. Among them, the ZnPc-1/ZnPc-4 heterojunction has the highest PCE value. So far, the best certified experimental efficiency of an organic solar cell is 12.7% (Ref. 32) and that of a single junction cell is 10–11%.[33] Moreover, these PCE values are comparable to the theoretical values of previously predicted bilayer phosphorene/MoS_2 (16–18%),[34] Edge-Modified phosphorene nanoflake heterojunctions,[35] Fullerene derivative (PBCM) and hexagonal BN and graphene (CBN) heterojunctions (10–20%),[36] g-SiC_2 based systems (12–20%),[37] and ZnPc/PSFP molecular heterojunctions (13–24.9%).[38]

The striking efficiency tunability found here is achieved by stacking 2D ZnPc semiconductors with different nitrogen content together. Nitrogen doping in 2D ZnPcs mainly results in shift of the conduction and valence band offsets. Since the donor and acceptor materials are 2D benzene sharing ZnPcs and their derivatives, the lattice mismatch and moiré effect[39] between them do not need to be considered here. More importantly, our material design strategies of self-assembly, heteroatom doping, and heterostructure by interlayer stacking can be universally extended to the countless 2D organic materials for photovoltaic devices. For instance, porphyrin based 2D organic single layer and multilayers and porphyrin/phthalocyanine based 2D organic heterojunctions are potential candidates and are still under investigation.

In summary, we presented an idea of solar cells based on organic 2D semiconductors and demonstrated the PCE up to 14.04%. The performance of the 2D organic solar cells can be tailored by the building molecule, heteroatom doping, functionalization, and interlayer stacking. Further high-throughput optimization, including suitable screening of 2D organic single layers, better interlayer matching, and better balancing the electronic structures of donor and acceptor organic materials, might even promote the PCE value to a

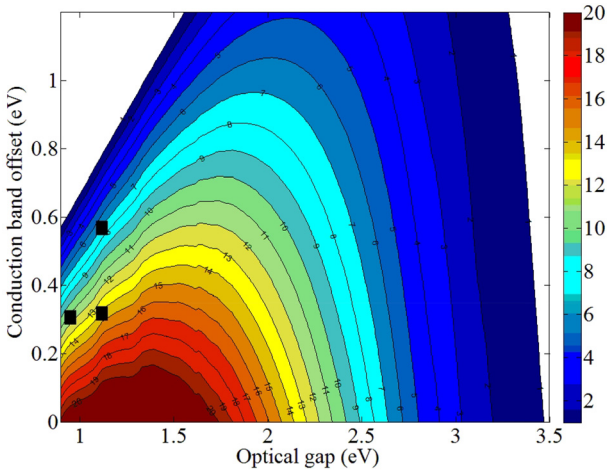


FIG. 4. Power conversion efficiency contour plot as a function of the 2D ZnPc donor optical bandgap and conduction band offset ΔE_c. Constant efficiency level curves up to 20% are shown here. The black cross shapes represent the efficiency limits of the three type-II alignments between 2D ZnPc-1 and 2D ZnPc-4, 2D ZnPc-1 and 2D ZnPc-5, and 2D ZnPc-4 and 2D ZnPc-5, respectively.

higher level. Combined with other advantages of organic PV and phthalocyanine based materials, the present results demonstrate that 2D ZnPcs are very promising for the next-generation organic solar cells.

See supplementary material for further details on atomic structures, AIMD simulation results, the proposed synthesis reaction schemes, band structures, binding energy, electrostatic potential, Fermi level, work function, and electron/hole mass.

This work was supported by the National Natural Science Foundation of China (11404050) and the Fundamental Research Funds for the Central Universities of China [DUT16RC(4)50, DUT16JJ(G)05, DUT16LAB01, and DUT17LAB19]. We also thank the Supercomputing Center of Dalian University of Technology for the computing resource.

[1]G. de la Torre, G. Bottari, and T. Torres, Adv. Energy Mater. **7**, 1601700 (2017).
[2]O. M. Yaghi, M. O'Keeffe, N. W. Ockwig, H. K. Chae, M. Eddaoudi, and J. Kim, Nature **423**, 705–714 (2003).
[3]N. W. Ockwig, O. Delgado-Friedrichs, M. O'Keeffe, and O. M. Yaghi, Acc. Chem. Res. **38**, 176–182 (2005).
[4]M. Abel, S. Clair, O. Ourdjini, M. Mossoyan, and L. Porte, J. Am. Chem. Soc. **133**, 1203–1205 (2011).
[5]C. G. Claessens, U. Hahn, and T. Torres, Chem. Rec. **8**, 75–97 (2008).
[6]D. Kearns and M. Calvin, J. Chem. Phys. **29**, 950 (1958).
[7]H. Kerp, H. Donker, R. Koehorst, T. Schaafsma, and E. Van Faassen, Chem. Phys. Lett. **298**, 302–308 (1998).
[8]G. Kresse and D. Joubert, Phys. Rev. B **59**, 1758–1775 (1999).
[9]P. E. Blöchl, Phys. Rev. B **50**, 17953–17979 (1994).
[10]J. P. Perdew, J. A. Chevary, S. H. Vosko, K. A. Jackson, M. R. Pederson, D. J. Singh, and C. Fiolhais, Phys. Rev. B **46**, 6671–6687 (1992).
[11]J. Heyd and G. E. Scuseria, J. Chem. Phys. **121**, 1187–1192 (2004).
[12]M. Gajdoš, K. Hummer, G. Kresse, J. Furthmüller, and F. Bechstedt, Phys. Rev. B **73**, 045112 (2006).
[13]F. Viñes, J. Carrasco, and S. T. Bromley, Phys. Rev. B **85**, 195425 (2012).
[14]K. Seiji, N. Takashi, and Y. Jun, J. Phys. Conf. Ser. **29**, 120 (2006).
[15]J. Zhou and Q. Sun, J. Am. Chem. Soc. **133**, 15113–15119 (2011).
[16]Y. Li, S. Zhang, J. Yu, Q. Wang, Q. Sun, and P. Jena, Nano Res. **8**, 2901–2912 (2015).
[17]L. E. Ramos, L. K. Teles, L. M. R. Scolfaro, J. L. P. Castineira, A. L. Rosa, and J. R. Leite, Phys. Rev. B **63**, 165210 (2001).
[18]N. T. Son, O. Kordina, A. O. Konstantinov, W. M. Chen, E. Sörman, B. Monemar, and E. Janzén, Appl. Phys. Lett. **65**, 3209–3211 (1994).
[19]J. Qiao, X. Kong, Z.-X. Hu, F. Yang, and W. Ji, Nat. Commun. **5**, 4475 (2014).
[20]K. Kaasbjerg, K. S. Thygesen, and A.-P. Jauho, Phys. Rev. B **87**, 235312 (2013).
[21]P. Wang, X. Jiang, and J. Zhao, J. Phys. Condens. Matter **28**, 034004 (2016).
[22]X. Jiang, P. Wang, and J. Zhao, J. Mater. Chem. A **3**, 7750–7758 (2015).
[23]M. V. Martinez-Diaz, G. de la Torre, and T. Torres, Chem. Commun. **46**, 7090–7108 (2010).
[24]N. Kobayashi, S. I. Nakajima, H. Ogata, and T. Fukuda, Chem. - Eur. J. **10**, 6294–6312 (2004).
[25]J. L. Sessler and D. Seidel, Angew. Chem. Int. Ed. **42**, 5134–5175 (2003).
[26]A. K. Geim and I. V. Grigorieva, Nature **499**, 419–425 (2013).
[27]Y. Han, Y. Liu, J. Yuan, H. Dong, Y. Li, W. Ma, S.-T. Lee, and B. Sun, ACS Nano **11**, 7215–7222 (2017).
[28]X. Wang and F. Xia, Nat. Mater. **14**, 264–265 (2015).
[29]M. Yang, L. Wang, T. Hou, and Y. Li, J. Mater. Chem. C **5**, 201–207 (2017).
[30]I. Gur, N. A. Fromer, M. L. Geier, and A. P. Alivisatos, Science **310**, 462–465 (2005).
[31]M. C. Scharber, D. Mühlbacher, M. Koppe, P. Denk, C. Waldauf, A. J. Heeger, and C. J. Brabec, Adv. Mater. **18**, 789–794 (2006).
[32]M. Li, K. Gao, X. Wan, Q. Zhang, B. Kan, R. Xia, F. Liu, X. Yang, H. Feng, W. Ni, Y. Wang, J. Peng, H. Zhang, Z. Liang, H.-L. Yip, X. Peng, Y. Cao, and Y. Chen, Nat. Photonics **11**, 85–90 (2017).
[33]J. Zhao, Y. Li, G. Yang, K. Jiang, H. Lin, H. Ade, W. Ma, and H. Yan, Nature Energy **1**, 15027 (2016).
[34]J. Dai and X. C. Zeng, J. Phys. Chem. Lett. **5**, 1289–1293 (2014).
[35]W. Hu, L. Lin, C. Yang, J. Dai, and J. Yang, Nano Lett. **16**, 1675–1682 (2016).
[36]M. Bernardi, M. Palummo, and J. C. Grossman, ACS Nano **6**, 10082–10089 (2012).
[37]L.-J. Zhou, Y.-F. Zhang, and L.-M. Wu, Nano Lett. **13**, 5431–5436 (2013).
[38]K. Tanikawa, K. Ohno, Y. Noda, S. Ono, R. Kuwahara, A. Takashima, M. Nakaya, and J. Onoe, Chem. Phys. Lett. **686**, 68–73 (2017).
[39]J. Kang, J. Li, S.-S. Li, J.-B. Xia, and L.-W. Wang, Nano Lett. **13**, 5485–5490 (2013).